Effect of erbium concentration on the Verdet constant dispersion of LiY1.0-xErxF4 single crystal

Effect of erbium concentration on the Verdet constant dispersion of LiY$_{1.0-x}$Er$_x$F$_4$ single crystal

YUKI TAMARU,[1,2,4] 🆔 HIKARU KUMAI,[1] ATSUSHI FUCHIMUKAI,[2]
HIYORI UEHARA,[1,3] TAISUKE MIURA,[2] AND RYO YASUHARA[1,3,5] 🆔

[1] *SOKENDAI (The Graduate University for Advanced Studies), 322-6 Oroshi-cho, Toki, Gifu 509-5292, Japan*
[2] *GIGAPHOTON INC., 400 Yokokurashinden, Oyama, Tochigi 323-8558, Japan*
[3] *National Institutes of Natural Sciences, National Institute for Fusion Science, 322-6 Oroshi-cho, Toki, Gifu 509-5292, Japan*
[4] *tamaru.yuki@nifs.ac.jp*
[5] *yasuhara@nifs.ac.jp*

Abstract: The dispersion of the Verdet constant of LiY$_{1.0-x}$Er$_x$F$_4$ crystals was evaluated from 190 nm to 500 nm for different doping concentrations of Er ions. A 15% doping concentration yielded a high Verdet constant of 54.5 rad/(T·m) at 193 nm. This value can be explained by the contribution of the diamagnetic term associated with LiYF$_4$ and the paramagnetic term of the Er ions. Although the LiYF$_4$ crystal yielded a lower value of −36.6 rad/(T·m) at 193 nm from Er-doped LiYF4, it can be used in the vacuum–ultraviolet region because of its high transmittance at wavelengths longer than 120 nm.

1. Introduction

The Faraday effect, a magneto-optic effect, is widely used in magnetic and electric current sensors and Faraday rotators (FRs). [1–3] The most important application for optical systems such as FRs is the optical isolator (OI), which is a polarization-dependent isolator for protecting light sources and preventing feedback to laser oscillators. The Faraday effect results in a rotation of the polarization plane of light traveling through a material when an external magnetic field is applied, and the rotation angle θ is expressed as

$$\theta = VHL, \tag{1}$$

where V is the Verdet constant and H is the strength of the magnetic field over the medium length L. The Verdet constant is material-specific and wavelength and temperature-dependent. A high V facilitates a reduction in the thickness of the media and strength of the external magnetic field. Ideal candidate materials for FRs should have both a high transmittance and a high Verdet constant V at the wavelength of the light source. For example, terbium gallium garnet (TGG) crystals are commonly used as FR materials at a wavelength of approximately 1000 nm ($V_{TGG} = 40$ rad/(T·m) at $\lambda = 1064$ nm) [4,5] and yttrium iron garnet (YIG) crystals are used at approximately 1500 nm ($V_{YIG} = 304$ rad/(T·m) at $\lambda = 1550$ nm). [6,7] These materials exhibit high Verdet constants in their respective wavelength regions, but cannot be used at wavelengths shorter than 390 nm due to their large absorptions. In the deep-ultraviolet ($\lambda = 193–300$ nm, DUV) and ultraviolet ($\lambda = 300–400$ nm, UV) regions, some materials have been reported as candidates for DUV-UV FRs. [8–12] For example, the Verdet constant is 70.1 rad/(T·m) at $\lambda = 193$ nm in synthetic quartz glass, 180 rad/(T·m) at $\lambda = 193$ nm in ADA crystal, and 74.5 rad/(T·m) at $\lambda = 193$ nm in DKDP crystal. In particular, LiREF$_4$ (RE = Tb, Dy, Ho, Er, and Yb) has been identified as a promising material because of its high Verdet constant, owing to the contribution of rare earth element

doping and short-wavelength absorption edge. For example, the Verdet constant of LiErF$_4$ with a short-wavelength absorption edge of 163 nm is 516 rad/(T·m) at $\lambda = 193$ nm and 279 rad/(T·m) at $\lambda = 248$ nm, which is suitable for constructing DUV FRs.

In this paper, we report the Er doping concentration dependence of the dispersion of the Verdet constant in LiY$_{1.0-x}$Er$_x$F$_4$. Non-doped LiYF$_4$ (YLF) is a well-known laser host material with a short-wavelength absorption edge of 120 nm. [13–15] This suggests that FRs can be constructed not only in the DUV region, but also in the vacuum ultraviolet (VUV) region below $\lambda = 200$ nm. Partially doped crystals (Er:YLF), which are known as laser active media at 551 nm and 2.8 μm [16–19] were also evaluated, because an enhancement in their magneto-optic properties was expected from the contribution of Er ions. In addition, the contribution of Er ions to the Verdet constant in the DUV region was evaluated by comparison with previous results for LiErF$_4$.

2. Experimental methods

The dispersion of the Verdet constant was measured using the polarization-stepping method. [20] The experimental setup is illustrated in Fig. 1. An optical discharge plasma light source (Energetiq Technology, Inc. EQ-99X LDLS) was used as the seed white light source ($\lambda = 170$–2100 nm). Two types of polarizers and spectrometers were used for accurate measurement in a wide wavelength region ($\lambda = 190$–500 nm). In the short-wavelength region ($\lambda = 193$–300 nm), a Wollaston-GlanTaylor polarizer (Kogakugiken Corp. WoG-193-E) and DUV spectrometer (Ocean insight Maya200) were used, whereas a GlanTaylor polarizer (Thorlabs, Inc. GL10) and a second spectrometer (Ocean Insight USB2000) were used in the long-wavelength region ($\lambda = 300$–500 nm). The sample was positioned, and an external magnetic field ($B = 1.18$ T at $L = 6$ mm, $B = 1.16$ T at $L = 10$ mm) was applied between the two polarizers. Two types of samples were measured: LiYF$_4$ (non-doped YLF, $L = 10$ mm) and LiY$_{0.85}$Er$_{1.5}$F4 (15% doped Er:YLF, $L = 6$ mm). One of the polarizers is rotated using a stepping motor with a sampling pitch of 1°. The intensity of the transmitted light without an applied external magnetic field can be expressed as follows:

$$I_N(\theta) = I_0 \cos^2(\theta + \theta_0) + I_{min}, \tag{2}$$

where I_0 is the maximum intensity, θ is the rotation angle of the polarizers, θ_0 is the angular difference between the two polarizers, and I_{min} is the minimum intensity. By applying a magnetic field to the sample, polarization rotation θ_F due to the Faraday effect is induced, and thus, the above equation becomes

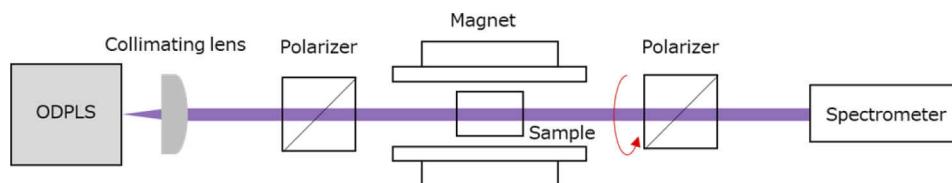$$I_B(\theta) = I_0 \cos^2(\theta + \theta_0 + \theta_F) + I_{min}. \tag{3}$$

Fig. 1. Experimental setup for measurement of the Verdet constant.

θ_F is determined by evaluating the phase difference between the two measurement data. From these data, the Verdet constant is derived using Eq. (1) for all wavelengths.

3. Result and discussion

Figure 2 shows the wavelength dependence of the Verdet constant and the transmittance in a non-doped YLF crystal. Figure 3 shows the results in a 15%-doped Er:YLF crystal. The gray

dotted lines indicate the wavelength of a typical DUV laser source. The Verdet constant exhibited opposite signs because Er ions are paramagnetic, whereas YLF crystals are diamagnetic. The Verdet constant dispersion of a diamagnetic material can be determined using the following equation [21]:

$$V_{dia}(\lambda) = -\frac{\pi}{\lambda}\frac{n^2 - 1}{2n}\left(A + \frac{B}{\lambda^2 - \lambda_0^2}\right),$$ (4)

where n is the refractive index, [22] λ_0 is the ultraviolet resonance wavelength, and $A = (1.21 \pm 0.02) \times 10^{-6}$ rad/T and $B = (1.55 \pm 0.06) \times 10^{-19}$ (rad·m^2)/T, $\lambda_0 = 39.7 \pm 0.2$ nm are the fitting parameters.
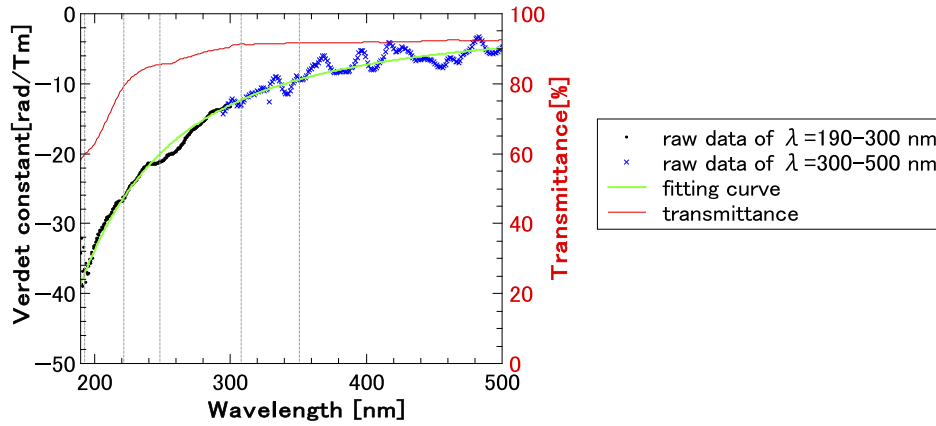

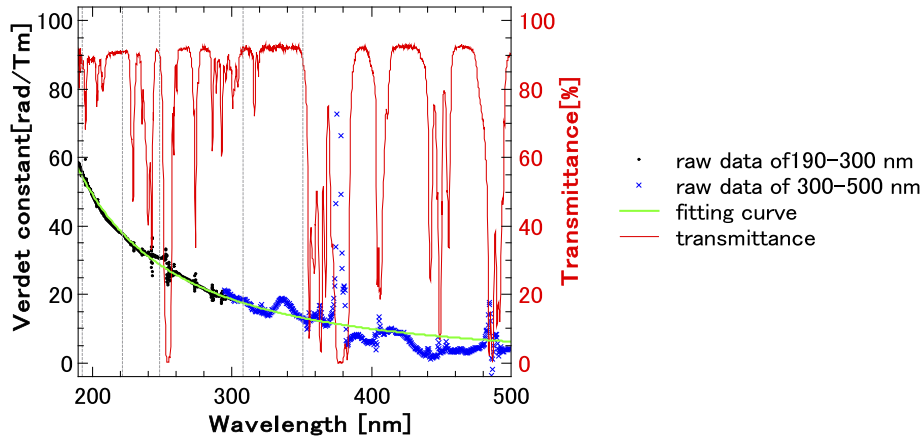**Fig. 2.** Dispersion of Verdet constant and transmittance in non-doped YLF.

Fig. 3. Dispersion of Verdet constant and transmittance in 15% doped Er:YLF.

Similarly, the properties of paramagnetic materials are given by the following equation [21]:

$$V_{para}(\lambda) = \frac{C}{T}\frac{(n+2)^2}{n}\frac{N}{\lambda_T^2 - \lambda^2},$$ (5)

where N is the number of atoms, T is the temperature, λ_T is the dominant wavelength transition, and C·N=-(54.4 ± 0.4)×10^{-18} (rad·m)/T and λ_T=100.3 ± 1.4 nm are the fitting parameters. The

fitting curve based on the preceding formula is represented by the solid lines in Figs. 2 and 3. YLF has a high transmittance in the entire UV-DUV region, but the Verdet constant is 36.6 rad/(T·m) at $\lambda = 193$ nm. The transmittance of the non-doped crystal is low, owing to the low purity of the crystal and its large length. For Er:YLF, although many absorption lines are associated with the absorption of Er ions, the Verdet constant is as high as 50 rad/(T·m) at $\lambda = 193$ nm at room temperature, and the FR can be constructed in $L = 15.7$ mm when the magnetic field is $B = 1$ T. Considering that the value is due to the contribution of the paramagnetic Er ions, it exhibits a higher V at lower temperatures, because the contribution of these ions is temperature-dependent. [21] In the region of the absorption lines, these properties fluctuate due to the contribution of electronic transitions. The slow fluctuation in the measurement results at $\lambda = 300$–500 nm (blue dot) is thought to be a measurement error caused by the birefringence of the crystals. Figure 4 shows the doping concentration dependence of the Verdet constant for typical excimer lasers that are widely used as DUV light sources. At all wavelengths, the magneto-optic properties are enhanced by increasing the Er doping concentration. The relationship between the doping concentration of Er ion x and the Verdet constant can be expressed using the following equation:

$$V_{LiY_{1.0-x}Er_xF_4}(x) = V_{LiYF_4} \times (1 - x) + V_{LiErF_4} \times x, \tag{6}$$

where V_{LiYF_4} is the Verdet constant of the non-doped YLF and V_{LiErF_4} is the Verdet constant of LiErF$_4$. The behavior of the Verdet constant at every wavelength can be explained. Table 1 lists the Verdet constants at each wavelength. LiErF$_4$, which has the highest concentration of Er, is suitable for constructing UV-DUV FRs because of its large Verdet constant, but it cannot be used as an F2 laser with a wavelength of 157 nm owing to Er ion absorption. In comparison, YLF crystals do not exhibit a large Verdet constant. However, their short-wavelength absorption edge is located at 120 nm, and the Verdet constant increases as it approaches the absorption edge. The value is predicted to be −63.7 rad/(T·m) at $\lambda = 157$ nm, which facilitates the construction of FRs in the VUV region, such as in the case of the F2 laser. Assuming a magnetic field strength of 1 T, the FR can be constructed with $L = 12.3$ mm. By controlling the doping concentration, it is possible to use this crystal for various wavelengths in the UV-VUV region.
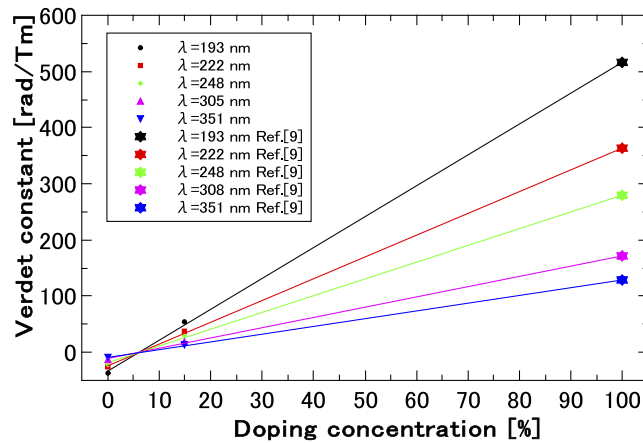

Fig. 4. Doping concentration dependence of Verdet constant of LiY$_{1.0-x}$Er$_x$F$_4$ for a typical DUV-excimer laser.

Table 1. Comparison of Verdet constants for several DUV-VUV excimer lasers

Laser type λ	XeF 351 nm	XeCl 308 nm	KrF 248 nm	KrCl 222 nm	ArF 193 nm	F2 157 nm
$LiYF_4$	−9.5	−12.9	−21.3	−26.4	−36.6	−63.7 (predicted)
$LiY_{0.85}Er_{0.15}F_4$	13.0	18.4	30.7	37.3	54.5	-
$LiErF_4$ [9]	128	171	279	363	516	-

4. Conclusion

The Verdet constant of $LiY_{1.0-x}Er_xF_4$ crystals with different doping concentration was measured over the range of 190–500 nm. To the best of our knowledge, this paper presents the first measurement of the Verdet constant of non-doped YLF. The measurements of partially doped Er:YLF crystals and previously reported data on $LiErF_4$ crystals revealed a relationship between the Er dopant concentration and the Verdet constant in the DUV region for the first time. In this region, crystals with a high Er doping concentration, which exhibited a high Verdet constant, were found to be suitable. However, non-doped YLF crystals can be used in the VUV region, which is shorter than the absorption edge (169 nm) of $LiErF_4$ crystals. For example, at 157 nm—the wavelength of the F2 excimer laser—the Verdet constant is predicted to be −63.7 rad/(T·m). $LiY_{1.0-x}Er_xF_4$ is a good candidate material for an FR in the DUV-VUV region.

Disclosures. The authors declare no conflicts of interest.

Data availability. Data underlying the results presented in this paper are not publicly available at this time but may be obtained from the authors upon reasonable request.

References

1. A. D. Buckingham and P. J. Stephens, "Magnetic optical activity," Annu. Rev. Phys. Chem. **17**(1), 399–432 (1966).
2. M. N. Deeter, A. H. Rose, and G. W. Day, "Fast, sensitive magnetic-field sensors based on the Faraday effect in YIG," J. Lightwave Technol. **8**(12), 1838–1842 (1990).
3. K. Bohnert, P. Gabus, J. Nehring, and H. Brändle, "Temperature and vibration insensitive fiber-optic current sensor," J. Lightwave Technol. **20**(2), 267–276 (2002).
4. C. B. Rubinstein, L. G. Van Uitert, and W. H. Grodkiewicz, "Magneto-optical properties of rare earth (III) aluminum garnets," J. Appl. Phys. **35**(10), 3069–3070 (1964).
5. Northrop Grumman Corporation, Fairview Park Drive, Falls Church, VA; 2980 (United States).
6. R. W. Cooper, W. A. Crossley, J. L. Page, and R. F. Pearson, "Faraday rotation in YIG and TbIG," J. Appl. Phys. **39**(2), 565–567 (1968).
7. A. Ikesue and Y. L. Aung, "Development of optical grade polycrystalline YIG ceramics for Faraday rotator," J. Am. Ceram. Soc. **101**(11), 5120–5126 (2018).
8. P. Molina, V. Vasyliev, E. G. Víllora, and K. Shimamura, "CeF_3 and PrF_3 as UV-visible Faraday rotators," Opt. Express **19**(12), 11786–11791 (2011).
9. V. Vasyliev, E. G. Villora, M. Nakamura, Y. Sugahara, and K. Shimamura, "UV-visible Faraday rotators based on rare-earth fluoride single crystals: LiREF_4 (RE = Tb, Dy, Ho, Er and Yb), PrF_3 and CeF_3," Opt. Express **20**(13), 14460–14470 (2012).
10. J. L. Dexter, J. Landry, D. G. Cooper, and J. Reintjes, "Ultraviolet optical isolators utilizing KDP-isomorphs," Opt. Commun. **80**(2), 115–118 (1990).
11. Y. Tamaru, H. Chen, A. Fuchimukai, H. Uehara, T. Miura, and R. Yasuhara, "Wavelength dependence of the Verdet constant in synthetic quartz glass for deep-ultraviolet light source," Opt. Mater. Express **11**(3), 814–882 (2021).
12. H. Nishioka, H. Hisano, T. Kaminaga, K. Ueda, and H. Takuma, "Development of the UV Faraday rotator," rle **12**(11), 660–662 (1984).
13. E. Garcia and R. R. Ryan, "Structure of the laser host material LiYF_4," Acta Crystallogr. C Cryst. Struct. Commun. **49**(12), 2053–2054 (1993).
14. Qishu Fang, Hongbing Chen, Fang Xu, Sujing Wang, Zhe Liang, and Chengyong Jiang, "Bridgman growth of LiYF_4 single crystal in nonvacuum atmosphere," Chin. Opt. Lett. **8**(11), 1071–1074 (2010).
15. T. M. Pollak, R. C. Folweiler, E. P. Chicklis, J. W. Baer, A. Linz, and D. Gabbe, "Properties and fabrication of crystalline fluoride materials for high power laser applications," *ASTM Special Technical Publications*, 1980, pp. 127–135.
16. R. Brede, T. Danger, E. Heumann, G. Huber, and B. Chai, "Room-temperature green laser emission of Er:LiYF4," Appl. Phys. Lett. **63**(6), 729–730 (1993).

17. F. Heine, E. Heumann, T. Danger, T. Schweizer, G. Huber, and B. Chai, "Green upconversion continuous wave Er^{3+}:$LiYF_4$ laser at room temperature," Appl. Phys. Lett. **65**(4), 383–384 (1994).

18. G. J. Kintz, R. Allen, and L. Esterowitz, "Cw and pulsed 2.8-μm laser emission from diode-pumped Er^{3+}:$LiYF_4$ at room temperature," Appl. Phys. Lett. **50**(22), 1553–1555 (1987).

19. F. Auzel, S. Hubert, and D. Meichenin, "Multifrequency room-temperature continuous diode and Ar* laser-pumped Er^{3+} laser emission between 2.66 and 2.85 μm," Appl. Phys. Lett. **54**(8), 681–683 (1989).

20. J. L. Flores and J. A. Ferrari, "Verdet constant dispersion measurement using polarization-stepping techniques," Appl. Opt. **47**(24), 4396–4399 (2008).

21. M. J. Weber, "Faraday rotator materials for laser systems," Proc. SPIE **0681**, 75–90 (1987).

22. N. P. Barnes and D. J. Gettemy, "Temperature variation of the refractive indices of yttrium lithium fluoride," J. Opt. Soc. Am. **70**(10), 1244–1247 (1980).